Separation and Purification Technology 209 (2019) 470–481

Contents lists available at ScienceDirect

Separation and Purification Technology

journal homepage: www.elsevier.com/locate/seppur

Micropollutant rejection of annealed polyelectrolyte multilayer based nanofiltration membranes for treatment of conventionally-treated municipal wastewater

S. Mehran Abtahi[a,b,c], Lisendra Marbelia[a], Abaynesh Yihdego Gebreyohannes[a], Pejman Ahmadiannamini[d], Claire Joannis-Cassan[c], Claire Albasi[c], Wiebe M. de Vos[b,*], Ivo F.J. Vankelecom[a]

[a] Centre for Surface Chemistry and Catalysis, Department of Molecular and Microbial Systems, KU Leuven, Celestijnenlaan 200F, PO Box 2461, 3001 Heverlee, Belgium
[b] Membrane Science and Technology, MESA+ Institute for Nanotechnology, University of Twente, Faculty of Science and Technology, P.O. Box 217, 7500 AE Enschede, The Netherlands
[c] Laboratoire de Génie Chimique, Université de Toulouse, CNRS, INPT, UPS, Toulouse, France
[d] FUJIFILM Electronic Materials Inc, 6550 South Mountain Road, Mesa, AZ 85212, USA

ARTICLE INFO

Keywords:
Nanofiltration
Polyelectrolyte multilayers
Thermal annealing
Salt-annealing
Micropollutants

ABSTRACT

The ever-increasing concentrations of micropollutants (MPs) found at the outlet of conventional wastewater treatments plants, is a serious environmental concern. Polyelectrolyte multilayer (PEM)-based nanofiltration (NF) membranes are seen as an attractive approach for MPs removal from wastewater effluents. In this work, PEMs of poly(allylamine hydrochloride) (PAH) and poly(acrylic acid) (PAA) were coated in a layer by layer (LbL) fashion on the surface of a polyacrylonitrile ultrafiltration support to obtain PEM-based NF membranes. The impact of PEM post-treatment, by applying salt and thermal annealing, was then investigated in terms of swelling, hydrophilicity, permeability, and ion rejection. While thermal annealing produced a more compact structure of PEM, it did not improve the ion rejection. Among the different salt concentrations examined for the salt-annealing process, the highest ion rejection was observed for $(PAH/PAA)_{15}$ membranes annealed in 100 mM $NaNO_3$, interestingly without any decrease in the water permeability. This membrane was studied for the rejection of four MPs including Diclofenac, Naproxen, 4n-Nonylphenol and Ibuprofen from synthetic secondary-treated wastewater, over a filtration time of 54 h. At an early stage of filtration, the membrane became more hydrophobic and a good correlation was found between the compounds hydrophobicity and their rejection. As the filtration continued until the membrane saturation, an increase in membranes hydrophilicity was observed. Hence, in the latter stage of filtration, the role of hydrophobic interactions faded-off and the role of molecular and spatial dimensions emerged instead in MPs rejection. To test the suitability of the membranes for the ease of cleaning and repeated use, the sacrificial PEMs and foulants were completely removed, followed by re-coating of PEMs on the cleaned membrane. The higher MPs rejection observed in salt-annealed membranes compared to the non-annealed counterparts (52–82% against 43–69%), accompanied with still low ion rejection, confirm the high potential of PEM post-treatment to achieve better performing PEM-based NF membranes.

1. Introduction

Micropollutants (MPs) are usually defined as “chemical compounds present at extremely low concentrations i.e. from ng L^{-1} to µg L^{-1} in the aquatic environment, and which, despite their low concentrations, can generate adverse effects for living organisms” [1]. Sources of MPs in the environment are diverse and many of those originate from mass-produced materials and commodities [2]. In conventional wastewater treatment plants (WWTPs), primary wastewater treatment uses the physical process of sedimentation to remove settleable suspended solids from wastewater. While, secondary wastewater treatment uses biological treatment to remove dissolved and fine suspended organic matter, and in some cases nutrients, from wastewater [3]. Hence, today’s WWTPs were never designed to remove MPs from municipal wastewater, and as a consequence, MP accumulation in water bodies is increasing [4]. Over the last few years, this has created concerns due to

* Corresponding author.
E-mail address: w.m.devos@utwente.nl (W.M. de Vos).

https://doi.org/10.1016/j.seppur.2018.07.071
Received 3 June 2018; Received in revised form 25 July 2018; Accepted 25 July 2018
Available online 26 July 2018

their potentially harmful effects on the aquatic environment towards humans. This has persuaded researchers to develop, or improve advanced (tertiary) treatment technologies to be placed after the secondary treatment for enhanced removal of MPs [5]. Moreover, environmental regulations have been prepared to establish a framework for a water protection policy, for example within the EU. The first list of the EU's environmental quality standards was published in 2008 under the Directive 2008/105/EC [6]. Five years later, the Directive 2013/39/EU was launched to update the previous documents [7]. This directive suggested the monitoring of 49 priority substances and 4 metals, and also proposed the first European Watch List which was then published in the Decision 2015/495/EU of 20 March 2015 [8]. This list comprises 17 organic compounds, named "contaminants of emerging concern (CECs)", unregulated pollutants, for which Union-wide monitoring data needs to be gathered for the purpose of supporting future prioritization exercises [9,10]. In addition to these compounds, there are many organic compounds that are still not listed in the European environmental regulations. According to the review paper of Sousa et al. [10], 28 organic MPs not listed in the European legislation, were found at concentrations above 500 ng L^{-1}. Therefore, more research about occurrence and fate is needed for many of these emerging compounds.

Frequently used options to remove MPs from municipal wastewater effluents are: advanced oxidation processes [11,12], adsorption processes [4,13], and membrane filtrations [14]. Of these options, the high-pressure membrane processes nanofiltration (NF) and reverse osmosis (RO) are of great interest because of their higher removal rate, modularity and the possibility to integrate them with other systems [15]. For several applications, such as wastewater reclamation, the high energy consumption, high capital investments and operational costs of RO membranes has led to the preferred use of NF membranes over RO membranes [14,16]. In the last decade, the development of better performing NF membranes by surface modification techniques like grafting and interfacial polymerization is seen [17,18]. Since these processes are costly, laborious and rely on environmentally unfriendly solvents [19], the method chosen for this study was layer by layer (LbL) deposition technique. In this approach, the membrane is alternatively exposed to polycations and polyanions, to build polyelectrolyte multilayers (PEMs) of a controllable thickness [20,21]. Based on previous works, we know that these PEM coatings lead to membranes with properties expected for NF membranes, such as a good retention for small organic molecules and some retention of mono and divalent salts [22,23]. Parameters, such as ionic strength, pH, charge density, and the type of polyelectrolytes, influence the LbL process and determine the final properties of the resulting PEMs [24–26]. Apart from that, the stability of PEMs should be taken into account. For example, some PEMs are commonly highly swollen in water or even removed at higher salt concentration [27–30]. To increase PEMs stability, thermal and salt annealing where here chosen as both are common approaches to PEM annealing, especially for studies aimed at the study of their materials properties. Moreover, both approaches are relatively mild, and are not expected to lead to any damage to the PEM coating or to the support membrane.

It has been demonstrated that thermal annealing (i.e. exposing the PEMs to heat for a defined period of time) of these weaker PEMs is able to lead to improved stability and robustness [27,31]. Heating of multilayers up to > 200 °C caused an amidization reaction between the COO^- groups of poly (acrylic acid) (PAA) and the NH_3^+ groups of poly (allyl amine) hydrochloride (PAH) to form amide (NHCO) cross-links that rigidify the multilayers [32]. Despite the PEMs' stability through covalent crosslinks, the best arrangement of the multilayers would not be as separated layers but as complexes, where there is a maximal compensation between the negative and positive charges. PEMs' rearrangement into denser complexes, could also provide more stability. Thermal annealing increases mobility of the polyelectrolytes allowing them to re-arrange in the films to find more convenient conformations [31]. In addition, post-treatment of the multilayers in salt solution, i.e. salt annealing, also brings significant variation of the multilayer structure [33]. The films can be annealed when they are immersed in salt solutions of higher concentrations [34]. According to Izumrudov and Sukhishvili [35], the stability of the multilayers composed of two polyacids poly(methacrylic acid) (PMAA) and PAA increased after annealing the PEMs in NaCl solutions [35]. Salt annealing enhances the mobility of polyelectrolyte chains that are otherwise "frozen" in place via numerous ion pairs cross-links [36]. Indeed, the salt ions compete with the polyelectrolyte ionic groups for binding sites. This competition can lead to dissociation of the polyelectrolyte ion pairs, and thus should increase the mobility of dissociated polyelectrolyte chains [37].

One of the major disadvantages of NF and RO based membrane processes is the production of a "concentrate" stream containing all retained compounds [38]. So far, some achievements have been reported for the treatment of membrane concentrates (mainly using advanced oxidation processes and adsorption with activated carbon [39,40]). These methods however have only been examined at laboratory or pilot-plant scales. Additionally, the high cost of these post-treatment processes can inhibit their wider implementation [41,42]. Thus, biological treatment of the concentrate has been lately taken into account by some scientists [43,44]. The main obstacle for a biological treatment of MP containing concentrates is their high salinities, i.e. above 1% (10 g L^{-1} NaCl), that can cause high osmotic stress for the involved microorganisms or the inhibition of the reaction pathways in the organic degradation process [45,46]. Indeed, the efficiency of MPs biodegradation drastically declines due to the high salt content of the concentrate steam [47–49]. In view of this, our recent studies focused on the application of LbL-made NF membranes for tertiary treatment of municipal wastewater [22,23]. In these studies, two weak oppositely-charged polyelectrolytes, PAH and PAA (Fig. 1S in supplementary data) were coated onto hollow fiber dense ultrafiltration (UF) membranes by dip-coating [21]. In contrast to available commercial NF membranes that combine high salts and MPs rejection, a unique membrane with a low salt rejection (~17% for NaCl) and a very promising removal of MPs (~44–77%) was obtained [22]. This membrane could thus remove MPs without producing a highly saline concentrate stream that would otherwise disrupt its biological treatment. Moreover, it does not considerably change the salt balance of the effluent, making it an ideal effluent for the irrigation of agricultural crops that are sensitive to the salinity balance of the water used [50,51].

Supplementary data associated with this article can be found, in the online version, at https://doi.org/10.1016/j.seppur.2018.07.071.

The aim of this investigation is to study the impact of thermal and salt-annealing processes on weak PEM-based membranes in terms of MPs removal from secondary-treated wastewater. PEMs composed of PAH and PAA were coated on the surface of flat-sheet polyacrylonitrile (PAN) UF membranes. The PEMs were then post-treated by thermal and/or salt annealing, and were carefully characterized before and after annealing by hydration ratio, hydrophobicity, permeability and ion rejection. Afterwards, the rejection behavior of the best membrane for the removal of four MPs (including 4n-Nonylphenol (listed in the Directive 2008/105/EC [6] and 2013/39/EU [7]), Diclofenac (listed in the Decision 2015/495/EU [8]), Naproxen and Ibuprofen (both not listed in the European legislations [10]) from synthetic secondary-treated wastewater was studied over the filtration time. As severe fouling would always be a large problem in the MP removal from wastewater, we additionally show that these membranes can be easily cleaned using a sacrificial layer approach. The fouled membranes were cleaned by a cleaning solution to release both the foulants and the sacrificial PEMs coating. The re-deposition of the same PEMs on the pre-rinsed membranes was subsequently performed.

2. Experimental

2.1. Chemicals

The polymer PAN (Mw = 150,000 Da) was obtained from Scientific Polymer Product Inc., USA. The solvent, dimethyl sulfoxide (DMSO) was purchased from Acros Organics, Belgium. Other chemicals including two weak polyelectrolytes (PAH with Mw = 15,000 g mol^{-1} and PAA with Mw = 15,000 g mol^{-1}), all salts ($CaCl_2{\cdot}2H_2O$, Na_2SO_4, NaCl, K_2HPO_4, $MgSO_4{\cdot}7H_2O$, $NaNO_3$), peptone, meat extract and urea were obtained from Sigma–Aldrich. The main supplier of all analytical-grade MPs, with the physico-chemical properties given in our previous study [22], was also Sigma-Aldrich.

2.2. Synthetic wastewater

Synthetic secondary-treated municipal wastewater was prepared according to the "OECD Guideline for Testing of Chemicals" [52,53]. This media contained 50 ± 2 mg L^{-1} of chemical oxygen demand (COD), 10 ± 1 mg L^{-1} of total nitrogen (TN) and 1 ± 0.1 mg P-PO_4^{3-} L^{-1}. Mother stock solutions of MPs were separately prepared in highly pure methanol at a concentration of 1 g L^{-1}, stored in 15-mL amber glass bottles and kept in a freezer (−18 °C). Daughter stock solutions of each MP were then prepared separately in Milli-Q water from their individual mother stock solutions. An appropriate amount of each MP was subsequently added to the synthetic wastewater to reach to the target concentration of MPs in the feed. Here, as discussed in our previous study [22], the final concentrations of Diclofenac, Naproxen, Ibuprofen and 4n-Nonylphenol were 0.5, 2.5, 40 and 7 μg/L, respectively, based on available data in literature about concentration of target MPs in effluents of conventional municipal WWTPs.

2.3. COD, TN, and P-PO_4^{3-} measurements

Feed samples were initially filtered through 0.70 μm glass fiber filters (VWR, 516-0348, France). The analysis was later carried out by means of HACH LANGE kits (LCI 500 for COD, LCK 341 for TN, LCK 304 for NH_3-N, and LCK 341 for *P-PO_4^{3}*) along with a DR3900 Benchtop VIS Spectrophotometer equipped with a HT200S oven (HACH LANGE, Germany). These parameters were measured in duplicate and the average values are reported.

2.4. Preparation of hydrolyzed PAN (PAN-H) membranes

According to the protocol described by Xianfeng Li et al. [54], PAN-H flat sheet membranes were prepared via the phase inversion method. In short, 15 wt% PAN was dissolved in DMSO overnight at ambient temperature. It was then degassed for 3 h and the bubble-free solution was cast on the smooth surface of a non-woven polypropylene/polyethylene (PP/PE) support (Novatexx 2471, Freudenberg, Germany) by an automated casting machine (Automatic Film Applicator, Braive Instruments) at 2.25 cm s^{-1} casting speed to form a 250 μm thick wet film. The solvent was allowed to evaporate for 60 S prior to immersing the film in demineralized water (as a non-solvent solution) for ~15 min. In order to provide the surface with a negative charge, membrane hydrolysis was performed i.e. PAN films were immersed in 10 wt% NaOH at 50 °C for 40 min while stirring at 100 rpm. Under alkaline condition, part of the –CN groups are converted into COO^-. The resulting PAN-H membranes were then washed with tap water to remove the remaining NaOH, and were stirred overnight in demineralized water at ambient temperature, and finally stored in demineralized water for further use.

2.5. Attenuated total reflectance (ATR)-Fourier transform infrared spectroscopy (FTIR)

ATR-FTIR was used to determine the functional groups present at the membrane surface, by collecting an infrared spectrum in the range 370–4000 cm^{-1} [55]. This method was used to confirm the hydrolysis of the PAN support into a negatively-charged membrane support (PAN-H). ATR-FTIR spectra of membranes were acquired using a spectrometer (Varian 670-IR, Varian Inc., USA) in absorbance mode. Two coupons per membrane were air-dried overnight prior to the measurements to minimize the effect of water. From each coupon, three points were selected and the average of absorbance values are reported.

2.6. Preparation of PEM-based membranes/silicon wafers

LbL deposition of oppositely-charged weak polyelectrolytes was performed by dip-coating [21]. The PAN-H membranes were first put into the background electrolyte solution (50 mM $NaNO_3$) for 15 min, in order to wash the pores [55]. Buildup of PEMs was then carried out by means of an automated dip-coating machine (HTML, Belgium) comprising four compartments: the 1st and 3rd compartments are for both polyelectrolytes and the 2nd and the 4th for rinsing solutions [56]. In a sequencial manner, PAN-H membranes were entirely immersed in a 0.1 g L^{-1} polycation solution (PAH) containing 5 mM $NaNO_3$ at pH 6 and at ambient temperature. After 30 min, membranes were put in a rinsing solution containing only $NaNO_3$ with an ionic strength and a pH similar to that of the coating solution for 15 min to remove any loosely bound polymer chains. To form the first bilayer of PAH/PAA, the membranes were dipped for 30 min in a 0.1 g L^{-1} polyanion solution (PAA) at pH 6 and an ionic strength of 5 mM $NaNO_3$ and rinsed again in a separate rinsing solution exactly as before. This pattern was repeated until the formation of the desired number of polycation/polyanion bilayers i.e. $(PAH/PAA)_n$ [23]. Selected PEM-based membranes were separately annealed in solutions of 50, 100 and 150 mM $NaNO_3$ for 20 h at room temperature [36,57]. The thermal annealing process was conducted by heating of some of the membranes to 60 °C for 5 h [58] in order to impose chemical crosslinking between the amine group and the carboxylic acid of the PAH and PAA polyelectrolytes, respectively [59].

In order to measure the dry and wet thicknesses of adsorbed polyelectrolytes (Section 2.7), the same deposition technique was also applied on the surface of silicon wafers, pre-treated by a 10-min plasma treatment using a low-pressure Plasma Etcher (JLS designs Ltd, UK), leading to a reproducible negative charge at the surface of all wafers. After coating, all samples were dried under a nitrogen stream prior to further measurements.

2.7. Spectroscopic ellipsometry

Dry and wet thicknesses of deposited multilayers on the surface of the plasma-treated silicon wafers were measured using an *in-situ* Rotating Compensator Spectroscopic Ellipsometer (M-2000X, J. A. Woollam Co, Inc.) operated in a wavelength range from 370 to 920 nm at incident angle of 70°. The wavelength range used was dictated by significant light absorption by the windows of the test cell below 370 nm, and by water absorption above 920 nm. The time resolution was around 2 s per full spectral scan, and the light spot size was about 2 mm. In the present study, the Cauchy model was used to fit to the ellipsometric parameters (Δ and ψ). The Cauchy model ($n(\lambda) = A + B/\lambda^2$, where A and B are the Cauchy parameters) describes how the refractive index (n) depends on the wavelength (λ), and is commonly used for thin polymeric coatings. Data obtained on three parts of each wafer were reported as a mean dry thickness ± standard deviation. By using Milli-Q water, and a Woollam wet cell, the wet thickness of the multilayers was also measured three times for each wafer. By dry and wet thicknesses, the hydration ratio was determined by Eq. (1) [60,61], and denotes the fraction of water in the layer.

$$Hydration\ \ ratio = \frac{d_{swollen} - d_{dry}}{d_{swollen}} \quad (1)$$

2.8. Contact angle

Optical contact angle measurements were performed using a Krüss goniometer (Drop Shape Analyzer DSA 10 Mk2) in order to investigate the membranes hydrophilicity. Sessile drops of 2 μL deionized water was used to measure the contact angle. These measurements were carried out at three locations per membrane coupon and the average and standard deviation are reported. The measurement was carried out five seconds after the bubble was placed on the surface of the membranes. The membranes' hydrophilicity was evaluated before, during and after filtration of the MP-bearing synthetic effluent. Clean and fouled membranes were dried for 24 h at room temperature (20 °C) before the contact angle measurements.

2.9. Membrane performance

The performance of the PEM-based membranes was tested using a high-throughput dead-end filtration system (HTML, Belgium) containing 16 filtration cells with 3.14 cm^2 membrane area each. The system was pressurized with nitrogen (2 bar), and the feed solution was constantly stirred at 600 rpm to minimize concentration polarization. Before filtration tests, membranes were initially equilibrated by filtering deionized water until the permeate stream would remain constant.

2.9.1. Water and solute permeability

In order to calculate the permeability ($L\,m^{-2}\,h^{-1}\,bar^{-1}$), Eq. (2) was used, where V is the permeate flowrate ($L\,h^{-1}$), A is the membrane area (m2), and P is the applied pressure (bar). From each type of membranes, two coupons were selected and the average permeability with standard deviations are reported.

$$Permeability = \frac{V}{A.\,P} \quad (2)$$

2.9.2. Salts retention

The concentrations of NaCl, Na_2SO_4 and Na_3PO_4 in the feed solutions were adjusted to 0.1 $g\,L^{-1}$ of each in mixed-salt solutions. To determine the anion concentrations, an ion chromatograph machine (Metrohm 883 Basic IC Plus, USA) equipped with an anion separation column (Metrosep A Supp 5–100/4.0, Metrohm, USA) and software MaglCnet 3.1 was used. The sample loop was 20 μL and a conductivity based detector was used. The chemical suppression was performed with 100 mM H_2SO_4 and a mobile phase of 5 mM Na_2CO_3/5 mM $NaHCO_3$ was applied at a flow rate of 1.0 ml min^{-1}. Furthermore, single-salt solutions containing 0.1 $g\,L^{-1}$ of $CaCl_2$ were also prepared. The concentration of $CaCl_2$ was measured with a conductivity meter (Consort C3010, Belgium). Finally, the retention value R was calculated according to Eq. (3), where C_p and C_f are the solute concentration in the permeate and feed, respectively. Each measurement was performed in duplicate and the average values with standard deviations are reported.

$$R = \left(1 - \frac{C_p}{C_f}\right) \times 100 \quad (3)$$

2.9.3. MPs retention and analysis

In the case of wastewater filtration for MP retention, membrane compaction was first performed at 2 bar for 2 h using demineralized water. Subsequently, the MPs-bearing synthetic effluent was filtrated for 54 h in order to provide sufficient membrane saturation to ensure steady state rejections. During the filtration, permeate and feed samples were collected after 2, 4, 7, 23, 27, 31, 46, 50 and 54 h. A large volume of the MPs-bearing feed solution was used. Throughout the filtration, there was no a significant change in the volume and MPs concentration in the feed solution. To minimize concentration polarization, the feed solution was constantly stirred at 600 rpm, and the filtration was performed by a relatively low flux.

For MP analysis, samples were shipped to the LaDrôme laboratory (France) in a freeze box for analysis within 24 h under the analyzing license of cofrac ESSAIS. A multi-detection procedure including Gas Chromatography (coupled with ECD/NPD mass spectrometry) and Liquid Chromatography (along with DAD, fluorescence, tandem mass spectrometry) was applied for all MPs with Limit of Quantification (LQ) of 0.01 μg/L for Diclofenac, Naproxen and Ibuprofen, and 0.04 μg/L for 4n-Nonylphenol. Each measurement was performed in duplicate and the average of rejections with standard deviations are reported.

2.10. Cleaning protocol of the fouled membrane

After filtration of MP-bearing wastewater for 54 h, a modified cleaning protocol adapted from Ilyas et al. [62] and Fujioka et al. [63] was applied in order to remove both the sacrificial PEMs and foulants. Ilyas et al. [62] have already concluded that (PAH/PAA) multilayers can act as sacrificial coatings allowing them to be easily cleaned. The fouled membrane was first rinsed with the rinsing solution (3 M $NaNO_3$, pH:3) in a dead-end mode at a low pressure (2 bar) for 180 min. Membrane samples were subsequently stored in a 50-mL glass beaker filled with the rinsing solution. This beaker was then immediately put in a simple water bath (at ~30 °C) for overnight. The membrane was then washed with Milli-Q water to remove residual cleaning solution. Removal of the PEMs and foulants was investigated by comparing the permeability before and after rinsing to see if the permeability could be restored to that of the pristine uncoated membrane. Finally, re-deposition of the same multilayer of (PAH/PAA) was manually performed on the cleaned membrane and permeability was again measured. (Because of the small size of the membrane coupons already used for the filtration, we were not able to use the dip-coating machine. That is why coupons were re-coated by using beakers filled with polyelectrolyte and rinsing solutions under identical conditions as for the dip-coating machine).

3. Results and discussion

In first part of this section, the PEMs and the PEM-based membranes are characterized using ellipsometric measurements, ATR-FTIR analysis and the contact angle. The second part deals with the performance of the PEM-based membranes, in terms of the permeability, salt and MP retention and cleanability.

As described in the experimental section, PEMs were deposited on the surface of PAN-H membranes to form $(PAH/PAA)_{15}$ and $(PAH/PAA)_{15}$-PAH multilayers to ensure that the separating membrane is dense and free of defects. In addition, these PEMs were coated on the surface of plasma-treated silicon wafers with the same preparation method. Afterwards, post-treatment of the PEM-based membranes/wafers was immediately performed. According to these procedures, four categories of membranes/wafers were finally produced and tested: (i) non-annealed, (ii) thermally-annealed, (iii) salt-annealed, and (iv) salt and thermally-annealed PEMs.

3.1. Properties of PEMs

3.1.1. Ellipsometric measurements

The thickness and water content of PEMs are important parameters particularly when the membrane surface modification is combined with other post-treatments [58]. In this study, the hydration ratio of PEMs deposited on the surface of plasma-treated silicon wafers were obtained using dry and wet ellipsometric thicknesses. Both the dry and wet thickness of the multilayers generally increased after additional coating

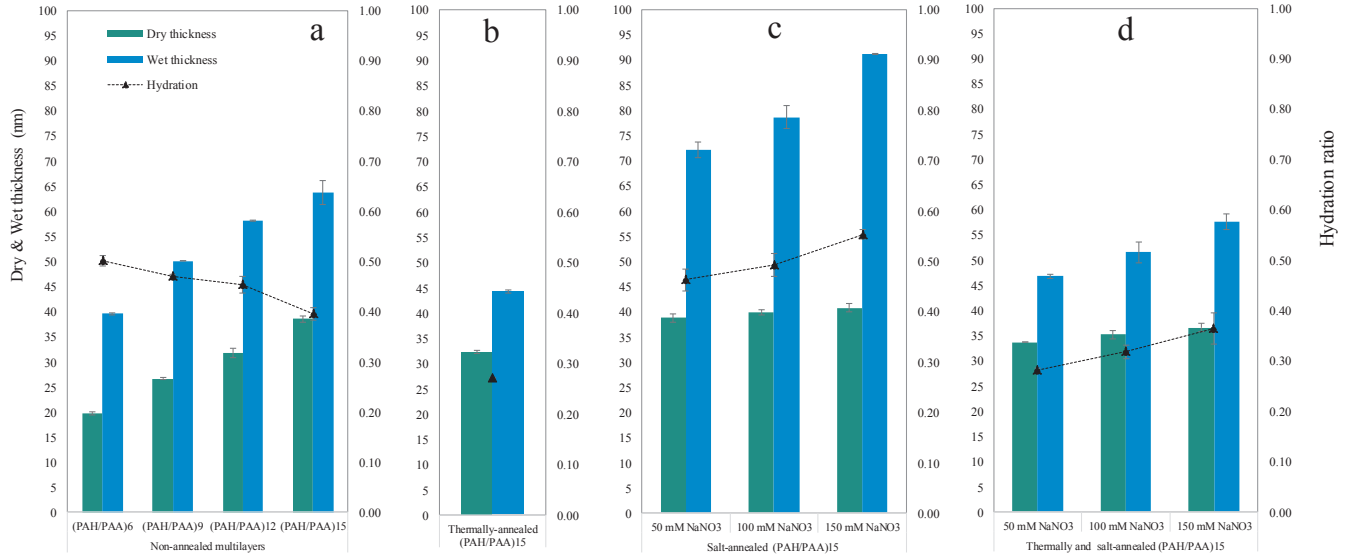

Fig. 1. Ellipsometric measurements of the coated silicon wafers of: (a) non-annealed, (b) thermally-annealed, (c) salt annealed and (d) thermally and salt-annealed PEMs.

steps, while a decreasing hydration ratio is observed (Fig. 1a). The build-up of these multilayers, prepared at an ionic strength of 5 mM $NaNO_3$ and pH 6 for both polyelectrolytes, follows a typical linear growth pattern, which was also found in previous study [22]. These results were then compared with salt and/or thermally annealed multilayes (Fig. 1b–d). By applying thermal annealing (Fig. 1b), the wet and dry thickness of $(PAH/PAA)_{15}$ multilayers decreased, but the wet thickness to a much larger extend, indicating that PEMs became more compact and less hydrated by thermal annealing. Upon salt annealing at various salt concentrations presented in Fig. 1c, the dry thickness remained nearly unaffected by increasing the salt concentration, while a slight increase in wet thickness was observed. Our data also indicate that the PEMs became more hydrated after annealing in salt solutions, the degree of which depends on the salt concentration [64]. To interpret this behavior, the type of dominant charge compensation of the multilayers should be taken into account. Schlenoff et al. [65,66] distinguished two kinds of charge compensation within the PEMs. When the charges of the polyelectrolyte are balanced by the oppositely charged polyelectrolyte, this is called “intrinsic charge compensation”. While, when the polyelectrolyte charges are balanced by counterions, this is called “extrinsic charge compensation” [65,66]. At low ionic strength that PEMs were made (i.e. 5 mM $NaNO_3$), the charge compensation of the polyelectrolytes is dominated by electrostatic interactions between the oppositely-charged polyelectrolytes (i.e. intrinsic charge compensation). This resulted in thin and dense multilayers with a relatively low mobility of the polymer chains. Upon post-treatment of PEMs at high ionic strengths (i.e. salt annealing), charge compensation by counterions is favored, shifting the equilibrium towards extrinsic charge compensation [65]. The transition from intrinsic to extrinsic charge compensation is accompanied by more hydrated multilayers [67]. Similarly, de Grooth et al. [68] observed that PEMs, built from polycation (poly(diallyldimethylammonium chloride) (PDADAMAC)) and a polyanion (poly(styrene sulfonate) (PSS), are relatively more open and hydrated at higher salt ionic strength due to the increase in extrinsic charge compensation [68]. As illustrated in Fig. 1d, applying both salt and thermal annealing substantially reduced the PEMs’ wet thickness. The lowest hydration ratio was found in salt and thermally-annealed $(PAH/PAA)_{15}$ multilayers. It seems that the thermal annealing step dominates the change in properties.

3.1.2. ATR-FTIR

To provide charge to the PAN membrane, a hydrolysis step was performed and checked with ATR-FTIR. As shown in Fig. 2S in Supplementary data, the hydrolysis with alkaline solution is mainly based on the conversion of nitrile groups (C≡N) on the PAN membrane surface first into amide groups ($CONH_2$), and then into carboxylate (COO^-) groups [69]. Fig. 3S in Supplementary data gives the ATR-FTIR spectra of the PAN and PAN-H membranes. The PAN membrane shows three main peaks at 1460, 2245 and 2362 cm^{-1}. These peaks correspond to the stretching vibrations of the CN groups of the PAN membrane support. After the hydrolysis, most of the CN groups were converted to COO− groups, as shown by lowering the intensity of peaks at 2245 and 2362 cm^{-1}. Additionally, a prominent peak at 1508 cm^{-1} can now be noticed, corresponding to the carbonyl (−C═O) bond in the COO^- groups [70]. No $CONH_2$ group peak (1570 cm^{-1}) [71] was present on the FTIR spectra. This indicates the preference for the COO^- groups over the $CONH_2$ groups. These results demonstrate the successful hydrolysis of the PAN membrane into a negatively-charged membrane.

3.1.3. Contact angle of PEM-based-membranes

Water contact angles of non-annealed and annealed PEM-based membranes are shown in Fig. 4S, and explained in Section 1S in Supplementary data. In short, after thermal annealing of $(PAH/PAA)_{15}$ multilayers, the contact angle increased to 66.3°, which shows a nearly hydrophobic surface. Diamanti et al. [31] observed a similar trend when they investigated the impact of thermal annealing on the wettability of alginate poly-L-lysine polyelectrolyte multilayers. This behavior was attributed to the restructuring of the PEMs from stratified multilayers to the formation of complexes between the oppositely charged polyelectrolytes [31]. Multilayers annealed at 150 mM $NaNO_3$, however, became more hydrophobic (61.9°) than those annealed at lower salt concentrations. Salt annealing enhances the mobility of polyelectrolyte chains in the structure of multilayers [36,37]. As a result, the multilayers and the top layer become more mixed, and the excess charge of the top layer declines, leading to an increase in hydrophobicity. The variation in wetting behavior of annealed multilayers is likely a consequence of the multilayers’ re-arrangement, which needs to be studied further in detail.

3.2. Performance of PEM-based membranes

3.2.1. Permeability

Fig. 2 shows the pure water permeability of bare and coated PAN-H

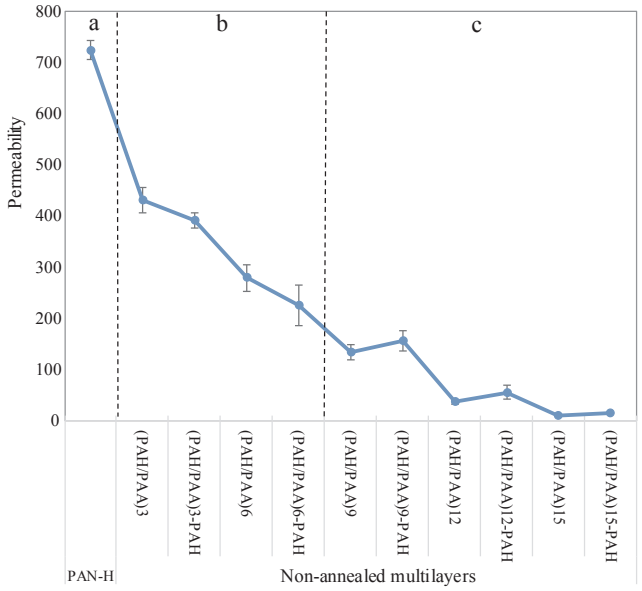

Fig. 2. Changes in the pure water permeability ($L\,m^{-2}\,h^{-1}\,bar^{-1}$) of the bare and coated membrane after deposition of (PAH/PAA) multilayers.

membranes. The permeability of the bare PAN-H membranes was $724\,L\,m^{-2}\,h^{-1}\,bar^{-1}$ (Fig. 2a). This value depends on the preparation condition and also the concentration of PAN in the casting solution [72]. For example, Hernalsteens [55] reported a pure water permeability of $890\,L\,m^{-2}\,h^{-1}\,bar^{-1}$ for PAN-H membranes prepared under similar conditions with this paper but at 13 wt% PAN concentration. By increasing the number of coated layers, the membrane permeability went down to 10.2 and 14.1 for $(PAH/PAA)_{15}$ and $(PAH/PAA)_{15}$-PAH membranes, respectively (Fig. 2b,c). These permeabilities are comparable to reported values for commercial NF membranes ($4.5–15.5\,L\,m^{-2}\,h^{-1}\,bar^{-1}$) [14], and did not significantly decline by further coating. Coating of PAN-H membranes with PAH/PAA bilayers were continued until the formation of 18 bilayers i.e. $(PAH/PAA)_{18}$. But, in terms of the water permeability, there was no a significant difference between the $(PAH/PAA)_{15}$ membranes and thicker ones. That is why, we chose $(PAH/PAA)_{15}$ and $(PAH/PAA)_{15}$-PAH membranes to perform other filtration experiments.

The permeability's downward trend, shown in Fig. 2, is also in agreement with the ellipsometry data of multilayers growth (Fig. 1a) and indicates that the addition of material on the membrane surface firstly decreases the membrane pore size (pore dominated regime) (Fig. 2b) and secondly comprises a thin film on top of the porous support (layer dominated regime) (Fig. 2c), leading to a decline in water permeability [68]. The swelling degree of the PEMs can also change the membrane permeability, whereby an increase in swelling leads to thicker but less dense polymer layers. PAH-terminated PEMs are more swollen than PAA-terminated layers [62]. Hence, in the case of thicker layers (Fig. 2c), the membrane permeability increased when PAH layers are coated and decreased again when PAA layers are applied. This zig-zag behavior (the flipping of the odd–even effect [68]) confirms that we are well within the layer dominated regime, and that any solute separation will be dominated by the PEM coating, rather than the original membrane pores.

Fig. 3 compares the permeability of the annealed and non-annealed PEM-based membranes. In general, there was no significant difference between them, but a glance at Fig. 3c,d demonstrates that an increase in swelling of the multilayer (Fig. 1c,d) leads to a more open layer and thus a higher permeability.

3.2.2. Salts rejection

PEM-based NF membranes are attractive for the separation of ions with different charges as well as for the size-selective separation of ions with the same charge [20]. As summarized in Table 1S in

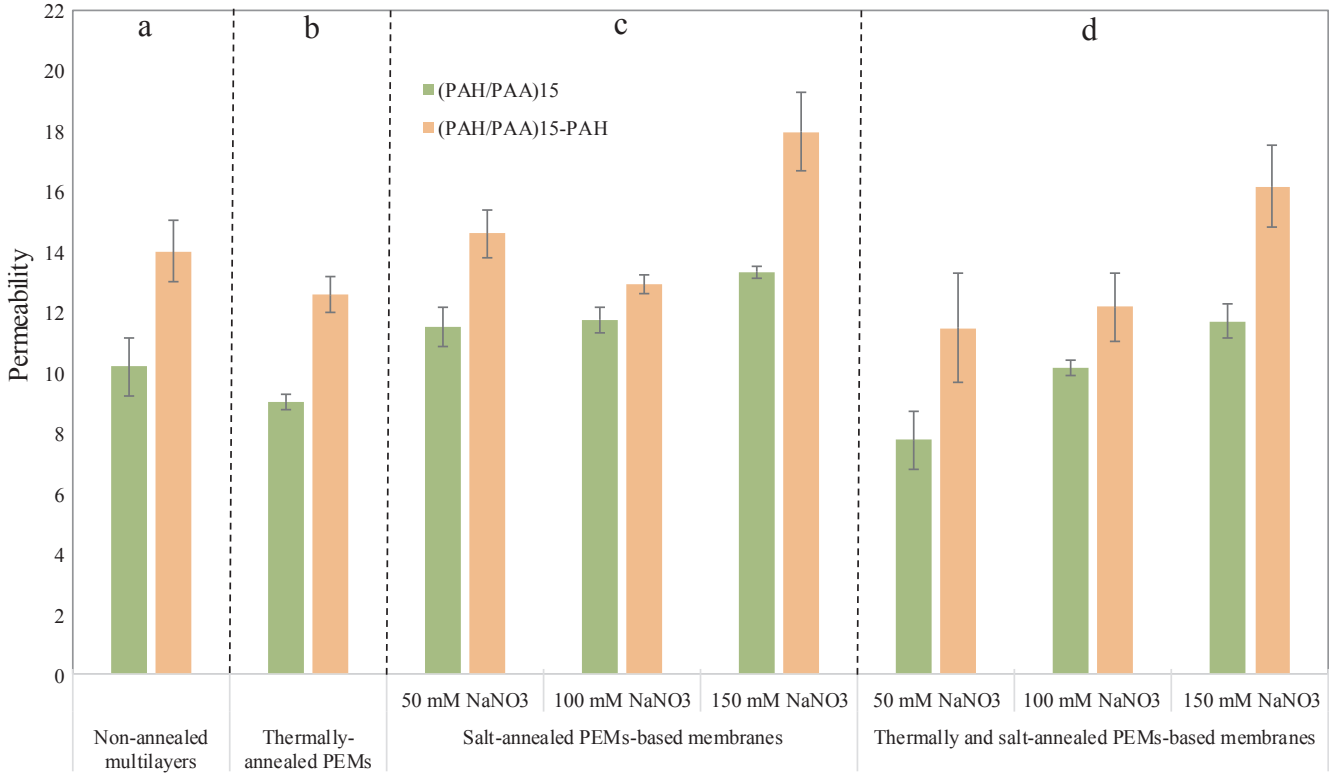

Fig. 3. Pure water permeability ($L\,m^{-2}\,h^{-1}\,bar^{-1}$) of (a) non-annealed, (b) thermally-annealed, (c) salt annealed, and (d) thermally and salt-annealed PEM-based membranes.

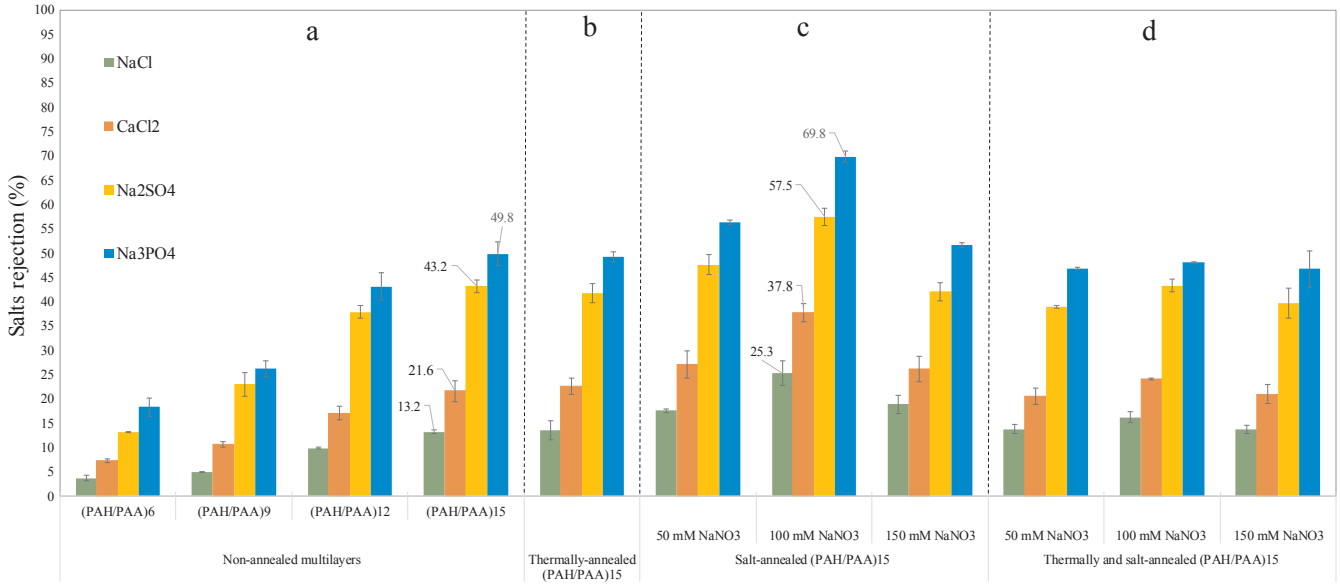

Fig. 4. Salts retention of the non-annealed and annealed $(PAH/PAA)_{15}$ membranes.

supplementary data, these membranes are recognized to have high rejections for divalent ions with low to moderate removal of monovalent ions, in particular when weak polyelectrolytes exist in the backbone of multilayers. In addition to size exclusion, charge exclusion plays a big role in solute rejection as the divalent ions are more charged than the monovalent resulting in a stronger repulsion [19,73].

To examine ion retention, filtration was performed using mixed-salt solutions containing NaCl, Na_2SO_4 and Na_3PO_4 (0.1 g L^{-1} each) and also single-salt solutions containing $CaCl_2$ (0.1 g L^{-1}). As the form of phosphate ion depends on the pH of the feed, the phosphate ions are present as HPO_4^{2-} (Fig. 5S in Supplementary data) [74]. Salt retentions of the annealed and non-annealed $(PAH/PAA)_{15}$ and $(PAH/PAA)_{15}$-PAH membranes are shown in Fig. 4 and Fig. 6S in supplementary data, respectively. For all membranes, in addition to the role of charge repulsion, the highest retentions were obtained for the large HPO_4^{2-}, followed by SO_4^{2-} and then Ca^{+2} and Cl^- at the last place, indicating that size exclusion plays an important role in their rejection. Fig. 4a and Fig. 6Sa show as the number of PAH/PAA bilayers were gradually elevated from 6 to 15, a considerable increment in salt rejection was noticed e.g. from 18.3% to 49.8% for HPO_4^{2-} retained by the PAA-terminated membranes. With more layers, less defects are present and the layer hydration is also lower.

Fig. 4b,d and Fig. 6Sb,d confirm that salts rejection did not improve with thermal annealing. Although thermal annealing could lead to denser multilayers (Fig. 1b,d) which would inevitably enhance the role of the size exclusion, it apparently reduces the charge of the top layer, leading to a reduction in the role of charge repulsion in salts rejection. Another reason might be the occurrence of defects in multilayers after applying the thermal annealing. The crosslinking (between the COO^- groups of PAA and the NH_3^+ groups of PAH [32]) can shrink the multilayers, and can impose stresses on the material, leading to create tiny cracks in the multilayers. This shows further optimization researches are still needed to find the proper degree and type of crosslinking process.

Regarding Fig. 4c & 6Sc, salt-annealed membranes performed better than non-annealed and thermally-annealed membranes for the purpose of ions retention. The highest salts retention was obtained for $(PAH/PAA)_{15}$ multilayers annealed in 100 mM $NaNO_3$. This membrane retained Na_3PO_4, Na_2SO_4, $CaCl_2$ and NaCl up to 69.8%, 57.5%, 37.8% and 25.3%, respectively. As seen in Section 3.1.1, a change in the charge compensation from intrinsic to extrinsic due to the salt annealing is accompanied by thicker, more hydrated and open layers [67]. This change will obviously affect the performance of PEM modified membranes. In line with the results of de Grooth et al. [68], at higher salt concentrations, thicker layers are formed on the membrane due to increased extrinsic charge compensation within the multilayers. These thicker layers result in an increased pore size decline and/or thicker PEMs on the membrane surface and as such a higher size exclusion [68]. Also, the shift from intrinsic to extrinsic charge compensation probably leads to an enhancement of the charge density of the PEMs. Then, the higher charge density of the layers results in membranes with better rejection properties for ions [75]. Furthermore, we see that the role of so-called "terminating layer's charge" is less pronounced in non-annealed membranes (compare Fig. 4c to Fig. 6Sc), while it is more apparent in salt-annealed membranes. For instance, on one hand, we do not see a substantial difference in rejection of the negative SO_4^{-2} or positive Ca^{+2} by both non-annealed negatively and positively-terminated membranes. On the other hand, retention of HPO_4^{-2} was observed by 69.8% for the salt-annealed PAA-terminated membranes (100 mM $NaNO_3$) compared to 54.7% for the salt-annealed PAH-terminated membranes. A converse behavior was observed for retention of Ca^{+2} i.e. 37.8% versus 48.4% for the salt-annealed PAA and PAH-terminated membranes, respectively. Consequently, for the non-annealed membranes, ion rejection is predominantly based on the ion size. While, in the case of salt-annealed counterparts, ion rejection is determined by the ion size followed by the surface charge of the multilayers.

While the focus so far has been on explaining the observed salt retentions, it should also be clear that $(PAH/PAA)_{15}$ membranes annealed in 100 mM $NaNO_3$ have good salt retention properties, while retaining a relatively high flux. For this membrane, a rejection of 69.8% for HPO_4^{2-} was obtained with a permeability of 11.8 L m^{-2} h^{-1} bar^{-1}, while its non-annealed counterpart showed retention and permeability of 54.7% and 10.2 L m^{-2} h^{-1} bar^{-1}, respectively. This shows the potential of PEMs annealing to design NF membranes and control their performance. The membrane with the highest ionic rejection was then tested for its MP removal.

3.2.3. MPs rejection

3.2.3.1. An overview of the MPs rejection by the NF membranes & general rejection mechanisms. Table 2S in Supplementary data presents some recent research data concerning the effectiveness of NF membranes in eliminating target MPs. To date, the rejection of uncharged MPs by NF membranes is considered to be predominantly caused by size exclusion, while charged molecules are also rejected by electrostatic interactions

with the charged membranes [76]. In this study, Diclofenac, Naproxen, and Ibuprofen are MPs with negative charge, while 4n-Nonylphenol is an uncharged compound at neutral pH [77].

Often, molecular weight is used to reflect molecular size. However, it does not truly reflect the size [78]. Consequently, spatial dimensions of MPs such as molecular width [79,80] and minimum projection area (MPA) [63,81] are also used to study the rejection behavior of NF membranes. MPA, as calculated from the van der Waals radius, is defined as the smallest two-dimensional projection area of a three-dimensional molecule. By projecting the molecule on an arbitrary plane, the two-dimensional projection area can be calculated and the process is repeated until the minimum projection area is obtained (Fig. 7S in Supplementary Data) [63].

When wastewater is used as feed solution, the existing interactions between the molecules and membranes may be influenced by the effluent organic matter. Then the separation mechanism of MPs cannot simply be attributed to the sieving effect and surface charge. In this case, hydrophobic interactions that take place between the fouled membrane surface and solutes can become dominant [82]. Regarding the hydrophilic or hydrophobic character of MPs, the octanol-water partition coefficient (K_{ow}) can be used as an indicator of hydrophobicity. Here, a pH-corrected value of log K_{ow}, known as log D, has been employed to predict the MPs' hydrophobicity. It can be defined as the K_{ow} ratio between the ionized and unionized form of the solute at a specific pH value (here the pH is adjusted at 7) [83]. Compounds with log D > 2.6 are referred as hydrophobic, and hydrophilic when log D ≤ 2.6 [84]. Hence, in the present work, using a synthetic wastewater effluent with neutral pH, Diclofenac, Naproxen and Ibuprofen are recognized as hydrophilic compounds (log_D: 1.77, 0.34 and 1.44, respectively [14]), while 4n-Nonylphenol (log_D: 6.14 [83]) is considered as a hydrophobic molecule.

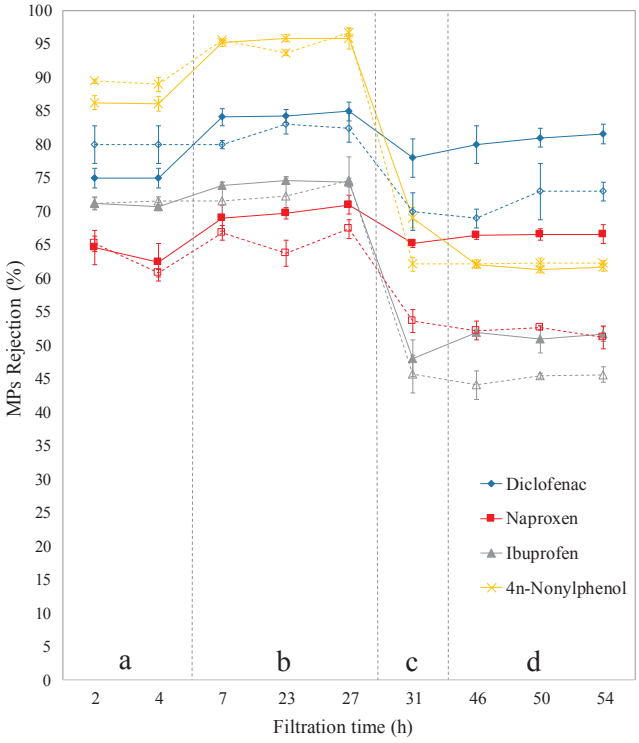

Fig. 5. Evolution of the MPs rejection over the filtration time (solid lines are related to the salt-annealed $(PAH/PAA)_{15}$ membranes annealed in 100 mM $NaNO_3$, while dashed lines indicate the performance of non-annealed $(PAH/PAA)_{15}$ membranes).

3.2.3.2. MPs rejection by non-annealed and salt-annealed PEM-based membranes. Higher ion rejection combined with a high flux, already shown in Fig. 3c and Fig. 4c, make the "salt-annealed $(PAH/PAA)_{15}$ membrane (annealed in 100 mM $NaNO_3$)" promising for the separation of MPs. According to the suggestions of Kimura et al. [85] and Yangali-Quintanilla et al. [78], and considering the very low concentrations of MPs in the effluent (0.5–40 $\mu g\,L^{-1}$), a long filtration duration of 54 h was applied to avoid overestimation of MP rejection (Fig. 5). First, the MP rejection increases over time (Fig. 5a,b). The apparent rejection of the hydrophobic 4n-Nonylphenol was the highest, followed by Diclofenac and then Ibuprofen and Naproxen. At this stage, Fig. 8S in supplementary data indicates a good correlation between the compounds' apparent rejection and their relevant hydrophobicity (logD). Also, there was no significant difference between the non-annealed and annealed membranes in MP rejection. At 31 h (Fig. 5c), we see a sudden reduction in retention of all MPs, the most severe for the hydrophobic 4n-Nonylphenol (e.g. from 95.9% to 69.1% for the salt-annealed membranes). In general, the continuous sorption process is usually characterized by the so-called "breakthrough curve", that is, a representation of the pollutant effluent concentration versus time profile [86]. In spite of still lack of a comprehensive knowledge about sorption capacity of PEM-based membranes, this rejection drop probably resembles the sharp effect of the breakthrough event on the MPs rejection. After membrane saturation, it maybe allows a higher amount of MPs to pass through the membrane leading to a reduction in the level of MPs rejection. As illustrated in Fig. 5d, a nearly stable retention of MPs was observed until the end of filtration process, whereby the steady-state rejection of Diclofenac, Naproxen, 4n-Nonylphenol and Ibuprofen were up to 81.5%, 66.6%, 61.7%, and 51.6%, respectively, for the salt-annealed membranes. Except for 4n-Nonylphenol, annealed membranes show better MP retention, compared to the non-annealed membranes. This is in a good agreement with the improved salt rejection observed in the previous section. It shows clearly that salt annealing can improve the rejection of specific organic compounds in PEM-based NF membranes. In Section 2S and Fig. 9S in supplementary data, contact angles of pristine and fouled membranes, along with its relation with MPs rejection, is discussed.

As seen in Fig. 5, as filtration time progresses, MPs rejection is likely to decline after the membrane is saturated upon long term operation. In other words, in line with Yangali-Quintanilla et al. [78], hydrophobic adsorption of MPs to the membrane was significant only in the first steps of wastewater filtration and it is less effective over time compared to the other rejection mechanisms. Regarding the importance of molecular dimensions and other physico-chemical properties in solutes rejection, the correlation between the steady-state rejection of MPs and such parameters is discussed in Section 3S in Supplementary Data.

3.2.3.3. Comparison with other tertiary treatment technologies. In order to compare our results with studies in the literature, Fig. 6 and Table 3S in Supplementary data have been prepared. Working on tertiary MPs removal is in its early days and it appears that there is a lack of comprehensive study in the literature. Considering this data, high MPs retentions would possibly enable these membranes to outperform current biological tertiary treatment methods (especially for the recalcitrant Diclofenac and Naproxen), and to compete with the available commercial NF and RO membranes for MPs removal from municipal effluents. Another priority of this membrane over the available commercial pressures-driven membranes is its lower salts rejection. Low salts rejection leads to the production of a concentrate stream with a low level of salinity. The biological treatment of the low-saline concentrate, will be more feasible in activated sludge-based reactors than the saline concentrates produced from commercial membranes [38,87–89]. Detrimental levels of the salinity on the performance of activated sludge reactors is discussed in our previous study [22]. Although the process of salt annealing slightly increases ion rejection (Fig. 4&6S), its rate of rejection is still too lower than what we see for both tight and loose NF membranes. For example, the rejections of NaCl and $MgSO_4$ by a tight NF90 membrane are reported up to

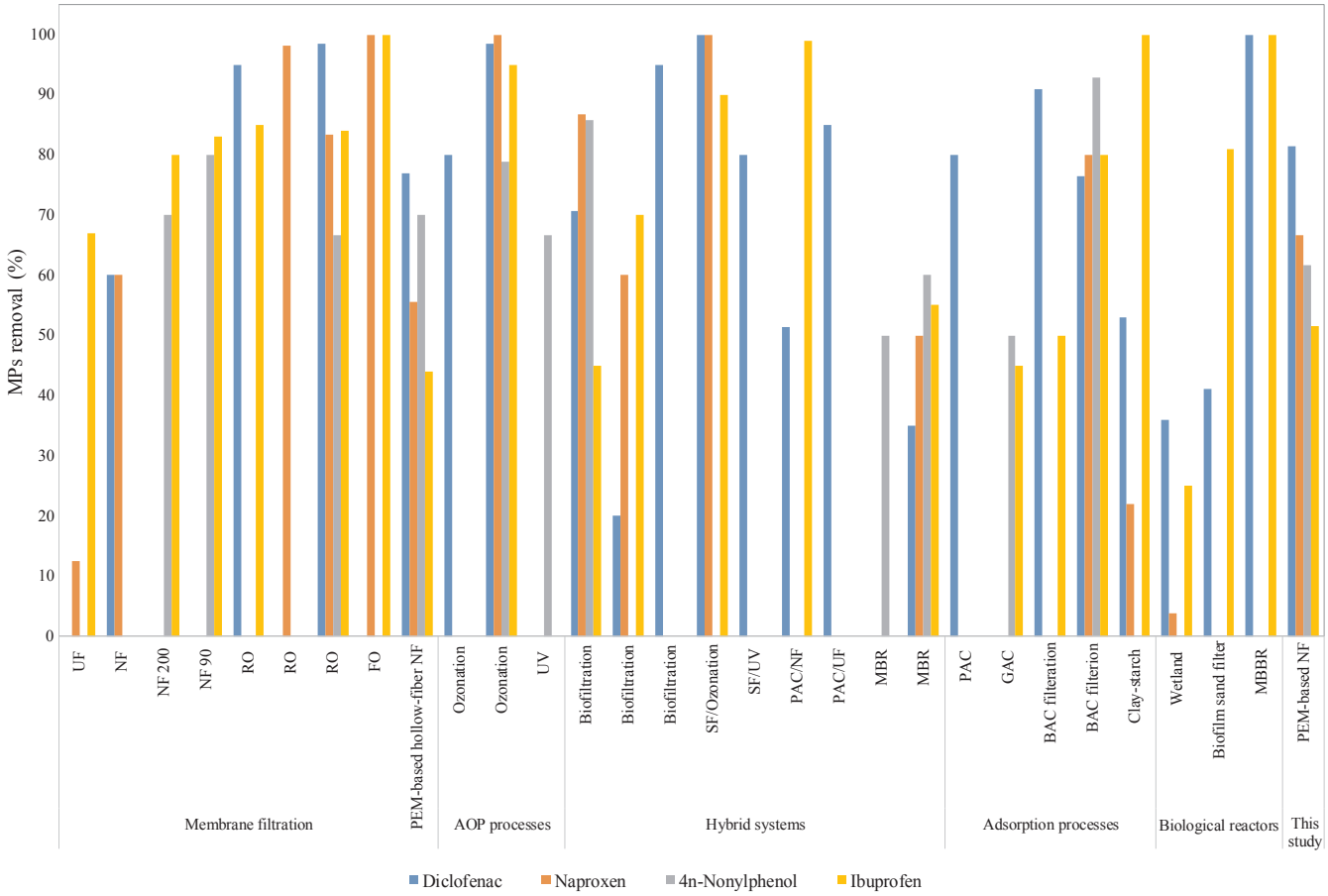

Fig. 6. Comparison of the steady-state rejection of MPs in this study with other tertiary treatment methods from the literature (More details are given in Table 3S in Supplementary data). (Abbreviations: AOP: advanced oxidation process, SF: sand filter, PAC: powdered activated carbon, GAC: granular activated carbon, MBBR: moving bed biofilm reactor, MBR: membrane bioreactor).

85–95% and 97–100%, respectively [90]. In the research of Levchenko and Freger [91] who studied the performance of NF membranes in salts rejection from secondary-treated municipal wastewater, loose NF270 membranes rejected NaCl, $MgCl_2$ and Na_2SO_4 up to around 60, 65 and 100%, respectively, while our salt-annealed membrane retained NaCl, $CaCl_2$ and Na_2SO_4 by around 25, 37 and 57%, respectively. This capability would be beneficial: i) when the concentrate stream is going to be treated by activated sludge-based reactors, and ii) when MPs removal is highly needed without or with a small change in salt balance of the effluent, to allow use for agricultural irrigation.

3.2.4. Membrane cleaning

In fouling studies related to the wastewater filtration, often, model foulants such as humic acids, bovine serum albumin (BSA), sodium alginate, and colloidal silica particles are used to simulate polysaccharide, refractory organic matter, protein and colloidal particles that are ubiquitous in secondary-treated wastewater [92]. The simplicity of those fouling systems probably leads to an unrealistic estimation of the MPs rejection by the clean and fouled membranes. Here, we used artificial wastewater, probably leading to a better judgement about the rejection behavior of membranes. But it also allows us to study another aspect of these multilayers, that they can be used as sacrificial layers to allow easy membrane cleaning [62,93].

In Fig. 7, the wastewater permeability of pristine and fouled salt-annealed $(PAH/PAA)_{15}$ membranes is shown at different cleaning steps. First of all, we evaluated whether the PEMs were completely removable by rinsing a pristine coated membrane with rinsing trigger solution (pH 3, 3 M NaCl) at 2 bar for 180 min. Indeed, the membrane permeability increased up to the level of a pristine uncoated membrane (~ 625 $L\,m^{-2}\,h^{-1}\,bar^{-1}$) (bar C). After filtration of MP-bearing wastewater, the membrane permeability of fouled membrane was about 4.6 $L\,m^{-2}\,h^{-1}\,bar^{-1}$ (bar D). Membrane cleaning with the rinsing solution at 2 bar for 180 min increased the permeability to ~170 $L\,m^{-2}\,h^{-1}\,bar^{-1}$, confirming the incomplete removal of the PEMs and foulants (bar E). Hence, an additional rinsing step was incorporated as described in experimental section i.e. immersion of pre-rinsed membrane in the same cleaning solution for overnight. This step resulted in an outstanding increase in the membrane permeability up to one that is nearly equal with the permeability of the pristine uncoated membrane (bar F). This demonstrates the full elimination of both sacrificial PEMs and foulants. Shan et al. [93] and Ilyas et al. [62] have successfully used a PEMs as both a sacrificial layer and as the separating layer of a NF membrane. They both could only completely remove all foulants by backwashing. Here, we could remove the PEMs along with attached foulants without employing any shear forces. Manual re-coating of the rinsed membrane with $(PAH/PAA)_{15}$ multilayers and its subsequent salt annealing in 100 mM $NaNO_3$ caused an evident reduction of the permeability that was roughly identical to the permeability of the pristine coated membrane (Part G). Our results demonstrate that the sacrificial layer approach is also promising in real wastewater applications.

4. Conclusion

Current municipal WWTPs were never designed for MP removal, and persistent MPs are still seen in the secondary-treated wastewater. The effect of thermal and salt-annealing was evaluated on the performance of polyacrylonitrile-supported NF membranes made from weak

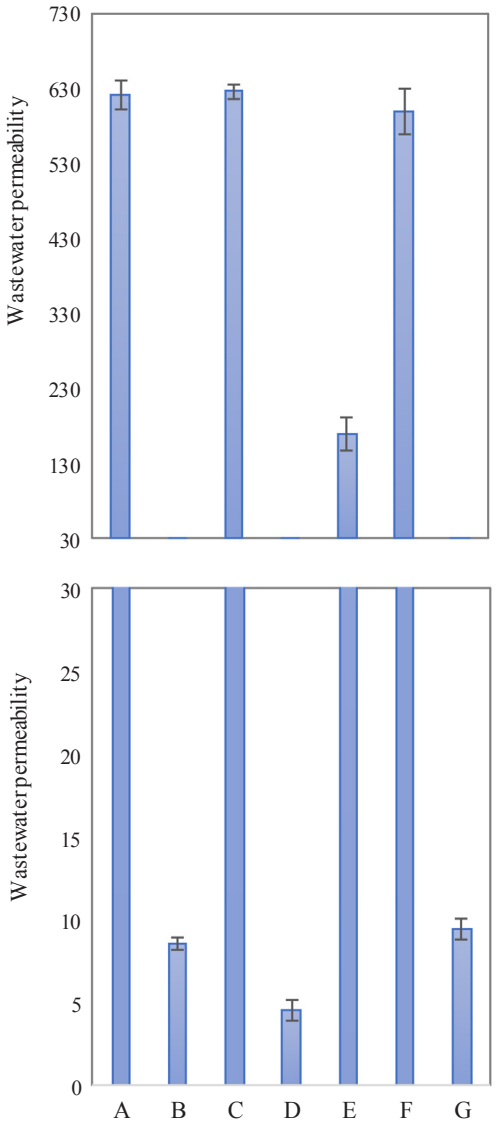

Fig. 7. MPs-bearing wastewater permeability ($L\,m^{-2}\,h^{-1}\,bar^{-1}$) of the salt-annealed $(PAH/PAA)_{15}$ membrane after the following steps: (A) uncoated pristine membrane; (B) pristine salt-annealed coated membrane; (C) rinsing of pristine coated membrane with cleaning solution for 180 min; (D) fouled salt-annealed coated membrane; (E) rinsing of fouled membrane with cleaning solution for 180 min; (F) rinsing of fouled membrane with cleaning solution for overnight; (G) regeneration of PEMs on the cleaned UF membrane.

PEMs for MPs polishing. In contrast to thermal annealing, salt annealing of PEMs enhanced salts rejection. The membrane also achieved a significantly improved rejection for some selected MPs. At initial steps of filtration, apparent rejections for both hydrophobic and hydrophilic MPs were governed by adsorption phenomena, whose role fade-away over time. The membrane then became more hydrophilic when steady-state rejection of MPs was achieved. Contribution of the molecular weight was higher than other dimensional parameters in steady-state rejection of all MPs by salt-annealed PEMs membranes, while MPA was a better surrogate parameter for the non-annealed membranes. A quite high removal of MPs next to the easy cleaning of both PEMs and foulants without employing any physical force are achievable in salt-annealed PEMs membranes, making them a promising technology for advanced wastewater treatment. These results were also accompanied with a relatively low salts rejection, allowing the production of low-saline concentrate streams that would make biological treatment much more straightforward.

Acknowledgments

The authors want to express their gratitude towards Benjamin Horemans, Peter Van den Mooter, Peter Salaets, and Muhammad Azam Rasool from the Faculty of Bioscience Engineering of KU Leuven. They also would like to deeply thank Mr. Thierry Trotouin from the Veolia Company for his continuous support and help. This project was accomplished under the framework of the EUDIME program (doctoral contract No. 2014-122), financially supported by the grant N. IOF-KP/13/004.

References

[1] J. Margot, Micropollutant Removal from Municipal Wastewater - From Conventional Treatments to Advanced Biological Processes, PhD thesis - Ecological Engineering Laboratory (ECOL) – Laboratory for Environmental Biotechnology (LBE)-Ecole Polytechnique Fédérale de Lausanne (EPFL), Switzerland, 2015.
[2] Y. Luo, W. Guo, H. Hao, L. Duc, F. Ibney, J. Zhang, S. Liang, X.C. Wang, A review on the occurrence of micropollutants in the aquatic environment and their fate and removal during wastewater treatment, Sci. Total Environ. 473–474 (2014) 619–641, https://doi.org/10.1016/j.scitotenv.2013.12.065.
[3] G. Tchobanoglous, F.L. Burton, H.D. Stansel, Wastewater Engineering: Treatment and Reuse, fourth ed., Metcalf & Eddy Inc by the McGraw Hill Companies, 2003, , https://doi.org/10.1016/0309-1708(80)90067-6.
[4] J. Margot, C. Kienle, A. Magnet, M. Weil, L. Rossi, L. Felippe, D. Alencastro, C. Abegglen, D. Thonney, N. Chèvre, M. Schärer, D.A. Barry, Treatment of micro-pollutants in municipal wastewater: Ozone or powdered activated carbon? Sci. Total Environ. 461–462 (2013) 480–498, https://doi.org/10.1016/j.scitotenv.2013.05.034.
[5] K. Arola, H. Hatakka, M. Mänttäri, M. Kallioinen, Novel process concept alternatives for improved removal of micropollutants in wastewater treatment, Sep. Purif. Technol. 186 (2017) 333–341, https://doi.org/10.1016/j.seppur.2017.06.019.
[6] The European Parliament and the Council of the European Union, Directive 2008/105/EC of 16 December 2008 on environmental quality standards in the field of water policy, amending and subsequently repealing Council Directives 82/176/EEC, 83/513/EEC, 84/156/EEC, 84/491/ECC, 86/280/ECC and amending Directive 2000/60/EC, Off. J. Eur. Union. 348 (2008) 84–97.
[7] The European Parliament and the Council of the European Union, Directives of 12 August 2013 amending Directives 2000/60/EC and 2008/105/EC as regards priority substances in the field of water policy, Off. J. Eur. Union. 226 (2013) 1–17.
[8] The European Parliament and the Council of the European Union, Decision 495/2015/EU of 20 March 2015 establishing a watch list of substances for Union-wide monitoring in the field of water policy pursuant to Directive 2008/105/EC of the European Parliament and of the Council, Off. J. Eur. Union. 78 (2015) 40–42.
[9] A.R. Ribeiro, O.C. Nunes, M.F.R. Pereira, A.M.T. Silva, An overview on the advanced oxidation processes applied for the treatment of water pollutants defined in the recently launched Directive 2013/39/EU, Environ. Int. 75 (2015) 33–51, https://doi.org/10.1016/j.envint.2014.10.027.
[10] J.C. Sousa, A. Ribeiro, M.O. Barbosa, M.F.R. Pereira, A.M.T. Silva, A review on environmental monitoring of water organic pollutants identified by EU guidelines, J. Hazard. Mater. 344 (2018) 146–162, https://doi.org/10.1016/j.jhazmat.2017.09.058.
[11] Y. Lee, D. Gerrity, M. Lee, A.E. Bogeat, E. Salhi, S. Gamage, R.A. Trenholm, E.C. Wert, S.A. Snyder, U. Von Gunten, Prediction of micropollutant elimination during ozonation of municipal wastewater effluents: use of kinetic and water specific information, Environ. Sci. Technol. 47 (2013) 5872–5881, https://doi.org/10.1021/es400781r.
[12] W. Yao, X. Wang, H. Yang, G. Yu, S. Deng, J. Huang, B. Wang, Y. Wang, Removal of pharmaceuticals from secondary effluents by an electro- peroxone process, Water Res. 88 (2016) 826–835, https://doi.org/10.1016/j.watres.2015.11.024.
[13] F. Bonvin, L. Jost, L. Randin, E. Bonvin, T. Kohn, Super-fine powdered activated carbon (SPAC) for efficient removal of micropollutants from wastewater treatment plant effluent, Water Res. 90 (2016) 90–99, https://doi.org/10.1016/j.watres.2015.12.001.
[14] M. Taheran, S.K. Brar, M. Verma, R.Y. Surampalli, T.C. Zhang, J.R. Valero, Membrane processes for removal of pharmaceutically active compounds (PhACs) from water and wastewaters, Sci. Total Environ. 547 (2016) 60–77, https://doi.org/10.1016/j.scitotenv.2015.12.139.
[15] J. Kim, P.-K. Park, C. Lee, H.-H. Kwon, S. Lee, A novel hybrid system for the removal of endocrine disrupting chemicals: nanofiltration and homogeneous catalytic oxidation, J. Memb. Sci. 312 (2008) 66–75, https://doi.org/10.1016/j.memsci.2007.12.039.
[16] F. Elazhar, J. Touir, M. Elazhar, S. Belhamidi, N. El Harrak, A. Zdeg, M. Hafsi, M. Taky, A. Elmidaoui, Techno-economic comparison of reverse osmosis and nanofiltration in desalination of a Moroccan brackish groundwater, Desalin. Water Treat. 55 (2015) 2471–2477, https://doi.org/10.1080/19443994.2014.959739.
[17] W.J. Lau, A.F. Ismail, Progress in interfacial polymerization technique on composite membrane preparation, in: 2nd Int. Conf. Environ. Eng. Appl., 2011, pp. 173–177.

[18] A.W. Mohammad, Y.H. Teow, W.L. Ang, Y.T. Chung, D.L. Oatley-radcliffe, N. Hilal, Nanofiltration membranes review: Recent advances and future prospects, Desalination 356 (2015) 226–254, https://doi.org/10.1016/j.desal.2014.10.043.
[19] R. Malaisamy, A. Talla-nwafo, K.L. Jones, Polyelectrolyte modification of nanofiltration membrane for selective removal of monovalent anions, Sep. Purif. Technol. 77 (2011) 367–374, https://doi.org/10.1016/j.seppur.2011.01.005.
[20] N. Joseph, P. Ahmadiannamini, H. Richard, I.F.J. Vankelecom, Layer-by-layer preparation of polyelectrolyte multilayer membranes for separation, Polym. Chem. 5 (2014) 1817–1831, https://doi.org/10.1039/c3py01262j.
[21] G. Decher, Fuzzy Nanoassemblies: Toward Layered Polymeric Multicomposites, Science (80-.) 277 (1997) 1232–1237, https://doi.org/10.1126/science.277.5330.1232.
[22] S.M. Abtahi, S. Ilyas, C. Joannis Cassan, C. Albasi, W.M. de Vos, Micropollutants removal from secondary-treated municipal wastewater using weak polyelectrolyte multilayer based nanofiltration membranes, J. Memb. Sci. 548 (2018) 654–666, https://doi.org/10.1016/j.memsci.2017.10.045.
[23] S. Ilyas, S.M. Abtahi, N. Akkilic, H.D.W. Roesink, W.M. de Vos, Weak polyelectrolyte multilayers as tunable separation layers for micro-pollutant removal by hollow fiber nanofiltration membranes, J. Memb. Sci. 537 (2017) 220–228, https://doi.org/10.1016/j.memsci.2017.05.027.
[24] K. Tang, N.A.M. Besseling, Formation of polyelectrolyte multilayers: ionic strengths and growth regimes, Soft Matter 12 (2016) 1032–1040, https://doi.org/10.1039/C5SM02118A.
[25] D. Kovacevic, S. Borkovic, J. Pozar, The influence of ionic strength, electrolyte type and preparation procedure on formation of weak polyelectrolyte complexes, Colloids Surfaces A Physicochem. Eng. Asp. 302 (2007) 107–112, https://doi.org/10.1016/j.colsurfa.2007.02.007.
[26] N. Wang, G. Zhang, S. Ji, Z. Qin, Z. Liu, The salt-, pH- and oxidant-responsive pervaporation behaviors of weak polyelectrolyte multilayer membranes, J. Memb. Sci. 354 (2010) 14–22, https://doi.org/10.1016/j.memsci.2010.03.002.
[27] K. Lin, Y. Gu, H. Zhang, Z. Qiang, B.D. Vogt, N.S. Zacharia, Accelerated amidization of branched poly(ethylenimine)/poly(acrylic acid) multilayer films by microwave, Heating (2016), https://doi.org/10.1021/acs.langmuir.6b02051.
[28] Y. Gu, E.K. Weinheimer, X. Ji, C.G. Wiener, N.S. Zacharia, Response of swelling behavior of weak branched poly(ethylene imine)/poly(acrylic acid) polyelectrolyte multilayers to thermal treatment, Langmuir 32 (2016) 6020–6027, https://doi.org/10.1021/acs.langmuir.6b00206.
[29] G.B. Sukhorukov, J. Schmitt, G. Decher, Reversible swelling of polyanion/polycation multilayer films in solutions of different ionic strength, PCCP 100 (1996) 948–953, https://doi.org/10.1002/bbpc.19961000642.
[30] J.J. Harris, M.L. Bruening, Electrochemical and in situ ellipsometric investigation of the permeability and stability of layered polyelectrolyte films, Langmuir 16 (2000) 2006–2013, https://doi.org/10.1021/la990620h.
[31] E. Diamanti, N. Muzzio, D. Gregurec, J. Irigoyen, M. Pasquale, O. Azzaroni, M. Brinkmann, S. Enrique, Impact of thermal annealing on wettability and antifouling characteristics of alginate poly-L-lysine polyelectrolyte multilayer films, Colloids Surfaces B Biointerfaces. 145 (2016) 328–337, https://doi.org/10.1016/j.colsurfb.2016.05.013.
[32] J.D. Mendelsohn, C.J. Barrett, V.V. Chan, A.J. Pal, A.M. Mayes, M.F. Rubner, Fabrication of microporous thin films from polyelectrolyte multilayers, Langmuir 16 (2000) 5017–5023, https://doi.org/10.1021/la000075g.
[33] X. Gong, C. Gao, Influence of salt on assembly and compression of PDADMAC/PSSMA polyelectrolyte multilayers, PCCP 11 (2009) 11577–11586, https://doi.org/10.1039/b915335g.
[34] R.A. McAloney, V. Dudnik, M.C. Goh, Kinetics of salt-induced annealing of a polyelectrolyte multilayer film morphology, Langmuir 19 (2003) 3947–3952, https://doi.org/10.1021/la026882s.
[35] V. Izumrudov, S.A. Sukhishvili, Ionization-controlled stability of polyelectrolyte multilayers in salt solutions, Langmuir 19 (2003) 5188–5191, https://doi.org/10.1021/la034360m.
[36] R.A. Ghostine, R.M. Jisr, A. Lehaf, J.B. Schlenoff, Roughness and salt annealing in a polyelectrolyte multilayer, Langmuir 29 (2013) 11742–11750, https://doi.org/10.1021/la401632x.
[37] T. Krebs, H.L. Tan, G. Andersson, H. Morgner, P. Gregory Van Patten, Increased layer interdiffusion in polyelectrolyte films upon annealing in water and aqueous salt solutions, PCCP 8 (2006) 5462–5468, https://doi.org/10.1039/b609440f.
[38] A. Kemperman, H. Temmink, A. Zwijnenburg, C. Kappel, H.H. Rijnaarts, K. Nijmeijer, Impacts of NF concentrate recirculation on membrane performance in an integrated MBR and NF membrane process for wastewater treatment, J. Memb. Sci. 453 (2014) 359–368, https://doi.org/10.1016/j.memsci.2013.11.023.
[39] A.Y. Bagastyo, J. Keller, Y. Poussade, D.J. Batstone, Characterisation and removal of recalcitrants in reverse osmosis concentrates from water reclamation plants, Water Res. 45 (2011) 2415–2427, https://doi.org/10.1016/j.watres.2011.01.024.
[40] A. Justo, Ó. González, J. Aceña, L. Mita, M. Casado, S. Pérez, B. Piña, C. Sans, D. Barceló, S. Esplugas, Application of bioassay panel for assessing the impact of advanced oxidation processes on the treatment of reverse osmosis brine, J. Chem. Technol. Biotechnol. 89 (2014) 1168–1174, https://doi.org/10.1002/jctb.4389.
[41] A. Pérez-Gonzalez, A.M. Urtiaga, R. Ibanez, I. Ortiz, State of the art and review on the treatment technologies of water reverse osmosis concentrates, Water Res. 46 (2012) 267–283, https://doi.org/10.1016/j.watres.2011.10.046.
[42] M.O. Barbosa, N.F.F. Moreira, A.R. Ribeiro, M.F.R. Pereira, A.M.T. Silva, Occurrence and removal of organic micropollutants: an overview of the watch list of EU Decision 2015/495, Water Res. 94 (2016) 257–279, https://doi.org/10.1016/j.watres.2016.02.047.
[43] U.E. Oviasogie, Continuous biological treatment of membrane concentrates of deinking wastewater streams from pulp and paper industry, J. Sci. Res. Reports. 2 (2013) 347–360, https://doi.org/10.9734/JSRR/2013/3714.
[44] R.M. Huang, J.Y. He, J. Zhao, Q. Luo, C.M. Huang, Fenton-biological treatment of reverse osmosis membrane concentrate from a metal plating wastewater recycle system, Environ. Technol. 32 (2011) 515–522, https://doi.org/10.1080/09593330.2010.504747.
[45] Y.C. Ching, G. Redzwan, Biological treatment of fish processing saline wastewater for reuse as liquid fertilizer, Sustainability 9 (2017) 1–26, https://doi.org/10.3390/su9071062.
[46] F. Kargi, A.R. Dinçer, Saline wastewater treatment by halophile-supplemented activated sludge culture in an aerated rotating biodisc contactor, Enzyme Microb. Technol. 22 (1998) 427–433, https://doi.org/10.1016/S0141-0229(97)00215-9.
[47] A.R. Dinçer, F. Kargi, Salt inhibition of nitrification and denitrification in saline wastewater, Environ. Technol. 20 (1999) 1147–1153, https://doi.org/10.1080/09593332008616912.
[48] M. Linaric, M. Markic, L. Sipos, High salinity wastewater treatment, Water Sci. Technol. 68 (2013) 1400–1405, https://doi.org/10.2166/wst.2013.376.
[49] T. Panswad, C. Anan, Specific oxygen, ammonia, and nitrate uptake rates of a biological nutrient removal process treating elevated salinity wastewater, Bioresour. Technol. 70 (1999) 237–243, https://doi.org/10.1016/S0960-8524(99)00041-3.
[50] R.D.H. Bugan, N.Z. Jovanovic, W.P. De Clercq, Quantifying the catchment salt balance: an important component of salinity assessments, S. Afr. J. Sci. 111 (2015) 1–8, https://doi.org/10.17159/sajs.2015/20140196.
[51] J.W. Kijne, Water and Salinity Balances for Irrigated Agriculture in Pakistan, 1996. doi: 10.3910/2009.006.
[52] C. Alcantara, R. Munoz, Z. Norvill, M. Plouviez, B. Guieysse, Nitrous oxide emissions from high rate algal ponds treating domestic wastewater, Bioresour. Technol. 177 (2015) 110–117, https://doi.org/10.1016/j.biortech.2014.10.134.
[53] OECD Guideline for the Testing of Chemicals, Simulation Test - Aerobic Sewage Treatment, Organisation for economic co-operation and development, Paris, 2001. doi:10.1787/9789264067394-eng.
[54] X. Li, S. De Feyter, D. Chen, S. Aldea, P. Vandezande, F. Du Prez, I.F.J. Vankelecom, Solvent-resistant nanofiltration membranes based on multilayered polyelectrolyte complexes, Chem. Mater. 20 (2008) 3876–3883, https://doi.org/10.1021/cm703072k.
[55] M. Hernalsteens, Biofouling in membrane bioreactors: Nexus between polyacrylonitrile surface charge and community composition, Master thesis, Center for surface chemistry and catalysis, University of KU Leuven, 2015.
[56] P. Ahmadiannamini, X. Li, W. Goyens, N. Joseph, B. Meesschaert, I.F.J. Vankelecom, Multilayered polyelectrolyte complex based solvent resistant nanofiltration membranes prepared from weak polyacids, J. Memb. Sci. 394–395 (2012) 98–106, https://doi.org/10.1016/j.memsci.2011.12.032.
[57] R.A. Ghostine, Ionic content and permeability of polyelectrolyte multilayers and complexes, PhD thesis, Department of Chemistry and Biochemistry, The Florida State University, 2013. https://www.engineeringvillage.com/share/document.url?mid=cpx_M37b8299515158e9263dM6fad10178163171&database=cpx.
[58] X. Zhu, D. Jańczewski, S.S.C. Lee, S.L.M. Teo, G.J. Vancso, Cross-linked polyelectrolyte multilayers for marine antifouling applications, ACS Appl. Mater. Interfaces 5 (2013) 5961–5968, https://doi.org/10.1021/am4015549.
[59] J. Park, J. Park, S.H. Kim, Cho Jinhan, Bang Joona, Desalination membranes from pH-controlled and thermally-crosslinked layer-by-layer assembled multilayers, J. Mater. Chem. 20 (2010) 2085–2091, https://doi.org/10.1039/b918921a.
[60] S. Dodoo, B.N. Balzer, T. Hugel, A. Laschewsky, R. Von Klitzing, S. Dodoo, B.N. Balzer, T. Hugel, A. Laschewsky, S. Dodoo, B.N. Balzer, T. Hugel, A. Laschewsky, R.V.O.N. Klitzing, Effect of ionic strength and layer number on swelling of polyelectrolyte multilayers in water vapour, Soft Mater. 4468 (2013), https://doi.org/10.1080/1539445X.2011.607203.
[61] S. Dodoo, R. Steitz, A. Laschewsky, R. Klitzing, Effect of ionic strength and type of ions on the structure of water swollen polyelectrolyte multilayers, PCCP 13 (2011) 10318–10325, https://doi.org/10.1039/c0cp01357a.
[62] S. Ilyas, J. De Grooth, K. Nijmeijer, W.M. De Vos, Multifunctional polyelectrolyte multilayers as nanofiltration membranes and as sacrificial layers for easy membrane cleaning, J. Colloid Interface Sci. 446 (2015) 386–393, https://doi.org/10.1016/j.jcis.2014.12.019.
[63] T. Fujioka, S.J. Khan, J.A. McDonald, L.D. Nghiem, Rejection of trace organic chemicals by a nanofiltration membrane: the role of molecular properties and effects of caustic cleaning, Desalination 368 (2015) 69–75, https://doi.org/10.1016/j.desal.2014.06.011.
[64] S.T. Dubas, J.B. Schlenoff, Swelling and smoothing of polyelectrolyte multilayers by salt, Langmuir 17 (2001) 7725–7727, https://doi.org/10.1021/la0112099.
[65] J.B. Schlenoff, H. Ly, M. Li, Charge and mass balance in polyelectrolyte multilayers, J. Am. Chem. Soc. 120 (1998) 7626–7634, https://doi.org/10.1021/ja980350+.
[66] T.R. Farhat, J.B. Schlenoff, Ion transport and equilibria in polyelectrolyte multilayers, Langmuir 17 (2001) 1184–1192, https://doi.org/10.1021/la001298+.
[67] J.B. Schlenoff, S.T. Dubas, Mechanism of polyelectrolyte multilayer growth: charge overcompensation and distribution, Macromolecules 34 (3) (2001) 592–598, https://doi.org/10.1021/ma0003093.
[68] J. de Grooth, R. Oborny, J. Potreck, K. Nijmeijer, W.M. de Vos, The role of ionic strength and odd-even effects on the properties of polyelectrolyte multilayer nanofiltration membranes, J. Memb. Sci. 475 (2015) 311–319, https://doi.org/10.1016/j.memsci.2014.10.044.
[69] Z.G. Wang, L.S. Wan, Z.K. Xu, Surface engineerings of polyacrylonitrile-based asymmetric membranes towards biomedical applications: an overview, J. Memb. Sci. 304 (2007) 8–23, https://doi.org/10.1016/j.memsci.2007.05.012.
[70] G. Zhang, H. Meng, S. Ji, Hydrolysis differences of polyacrylonitrile support membrane and its influences on polyacrylonitrile-based membrane performance,

Desalination 242 (2009) 313–324, https://doi.org/10.1016/j.desal.2008.05.010.
[71] W. Bao, Z. Xu, H. Yang, Electrokinetic and permeation characterization of hydrolyzed polyacrylonitrile (PAN) hollow fiber ultrafiltration membrane, Sci. China, Ser. B Chem. 52 (2009) 683–689, https://doi.org/10.1007/s11426-009-0064-5.
[72] N. Scharnagl, H. Buschatz, Polyacrylonitrile (PAN) membranes for ultra- and microfiltration, Desalination 139 (2001) 191–198, https://doi.org/10.1016/S0011-9164(01)00310-1.
[73] L. Ouyang, R. Malaisamy, M.L. Bruening, Multilayer polyelectrolyte films as nanofiltration membranes for separating monovalent and divalent cations, J. Memb. Sci. 310 (2008) 76–84, https://doi.org/10.1016/j.memsci.2007.10.031.
[74] P. Ahmadiannamini, X. Li, W. Goyens, B. Meesschaert, I.F.J. Vankelecom, Multilayered PEC nanofiltration membranes based on SPEEK/PDDA for anion separation, J. Memb. Sci. 360 (2010) 250–258, https://doi.org/10.1016/j.memsci.2010.05.021.
[75] L. Krasemann, B. Tieke, Selective ion transport across self-assembled alternating multilayers of cationic and anionic polyelectrolytes, Langmuir 16 (2000) 287–290, https://doi.org/10.1021/la991240z.
[76] S.O. Ganiyu, E.D. Van Hullebusch, M. Cretin, G. Esposito, M.A. Oturan, Coupling of membrane filtration and advanced oxidation processes for removal of pharmaceutical residues: a critical review, Sep. Purif. Technol. 156 (2015) 891–914, https://doi.org/10.1016/j.seppur.2015.09.059.
[77] V. Yangali-quintanilla, S.K. Maeng, T. Fujioka, M. Kennedy, Z. Li, G. Amy, Nanofiltration vs. reverse osmosis for the removal of emerging organic contaminants in water reuse, Desalin Water Treat. 34 (2011) 50–56 10/5004/dwt.2011.2860.
[78] V. Yangali-quintanilla, A. Sadmani, M. Mcconville, M. Kennedy, G. Amy, Rejection of pharmaceutically active compounds and endocrine disrupting compounds by clean and fouled nanofiltration membranes, Water Res. 43 (2009) 2349–2362, https://doi.org/10.1016/j.watres.2009.02.027.
[79] Y. Kiso, K. Muroshige, T. Oguchi, T. Yamada, M. Hhirose, T. Ohara, T. Shintani, Effect of molecular shape on rejection of uncharged organic compounds by nanofiltration membranes and on calculated pore radii, J. Memb. Sci. 358 (2010) 101–113, https://doi.org/10.1016/j.memsci.2010.04.034.
[80] H.T. Madsen, E.G. Søgaard, Applicability and modelling of nanofiltration and reverse osmosis for remediation of groundwater polluted with pesticides and pesticide transformation products, Sep. Purif. Technol. 125 (2014) 111–119, https://doi.org/10.1016/j.seppur.2014.01.038.
[81] T. Fujioka, S.J. Khan, J.A. McDonald, L.D. Nghiem, Nanofiltration of trace organic chemicals: a comparison between ceramic and polymeric membranes, Sep. Purif. Technol. 136 (2014) 258–264, https://doi.org/10.1016/j.seppur.2014.08.039.
[82] J. Garcia-Ivars, L. Martella, M. Massella, C. Carbonell-Alcaina, M.I. Alcaina-Miranda, M.I. Iborra-Clar, Nanofiltration as tertiary treatment method for removing trace pharmaceutically active compounds in wastewater from wastewater treatment plants, Water Res. 125 (2017) 360–373, https://doi.org/10.1016/j.watres.2017.08.070.
[83] H.Q. Dang, L.D. Nghiem, W.E. Price, Factors governing the rejection of trace organic contaminants by nanofiltration and reverse osmosis membranes, Dasalination Water Treat. 52 (2014) 589–599.
[84] R.V. Linares, V. Yangali-quintanilla, Z. Li, G. Amy, Rejection of micropollutants by clean and fouled forward osmosis membrane, Water Res. 45 (2011) 6737–6744, https://doi.org/10.1016/j.watres.2011.10.037.
[85] K. Kimura, G. Amy, J. Drewes, Y. Watanabe, Adsorption of hydrophobic compounds onto NF/RO membranes: an artifact leading to overestimation of rejection, J. Memb. Sci. 221 (2003) 89–101, https://doi.org/10.1016/S0376-7388(03)00248-5.
[86] H. Patel, R.T. Vashi, Fixed-bed column studies of dyeing mill wastewater treatment using naturally prepared adsorbents, in: Chapter 5., Charact. Treat. Text. Wastewater, Elsevier Inc., 2015, pp. 127–145. 10.1016/B978-0-12-802326-6.00005-8.
[87] P. Chelme-ayala, D.W. Smith, M.G. El-din, Membrane concentrate management options: a comprehensive critical review, Can. J. Civ. Eng. 36 (2009) 1107–1119, https://doi.org/10.1139/L09-042.
[88] P. Liu, H. Zhang, Y. Feng, F. Yang, J. Zhang, Removal of trace antibiotics from wastewater: a systematic study of nanofiltration combined with ozone-based advanced oxidation processes, Chem. Eng. J. 240 (2014) 211–220, https://doi.org/10.1016/j.cej.2013.11.057.
[89] Z. Jeirani, A. Sadeghi, J. Soltan, B. Roshani, B. Rindall, Effectiveness of advanced oxidation processes for the removal of manganese and organic compounds in membrane concentrate, Sep. Purif. Technol. 149 (2015) 110–115, https://doi.org/10.1016/j.seppur.2015.05.009.
[90] J. Radjenovic, M. Petrovic, F. Ventura, D. Barcelo, Rejection of pharmaceuticals in nanofiltration and reverse osmosis membrane drinking water treatment, Water Res. 42 (2008) 3601–3610, https://doi.org/10.1016/j.watres.2008.05.020.
[91] S. Levchenko, V. Freger, Breaking the symmetry: mitigating scaling in tertiary treatment of waste effluents using a positively charged nanofiltration membrane, Environ. Sci. Technol. 3 (2016) 339–343, https://doi.org/10.1021/acs.estlett.6b00283.
[92] L.D. Nghiem, P.J. Coleman, C. Espendiller, Mechanisms underlying the effects of membrane fouling on the nanofiltration of trace organic contaminants, Desalination 250 (2010) 682–687, https://doi.org/10.1016/j.desal.2009.03.025.
[93] W. Shan, P. Bacchin, P. Aimar, M.L. Bruening, V.V. Tarabara, Polyelectrolyte multilayer films as backflushable nanofiltration membranes with tunable hydrophilicity and surface charge, J. Memb. Sci. 349 (2010) 268–278, https://doi.org/10.1016/j.memsci.2009.11.059.